Electronic Supplementary Material (ESI) for Materials Chemistry Frontiers.

A Family of ssa-Type Copper-Based MOFs Constructed from Unsymmetrical Diisophthalates: Synthesis, Characterization and Selective Gas Adsorption

Fengli Chen, Dongjie Bai, Yao Wang, Donghao Jiang, Yabing He*

College of Chemistry and Life Sciences, Zhejiang Normal University, Jinhua 321004, China. E-mail: heyabing@zjnu.cn.

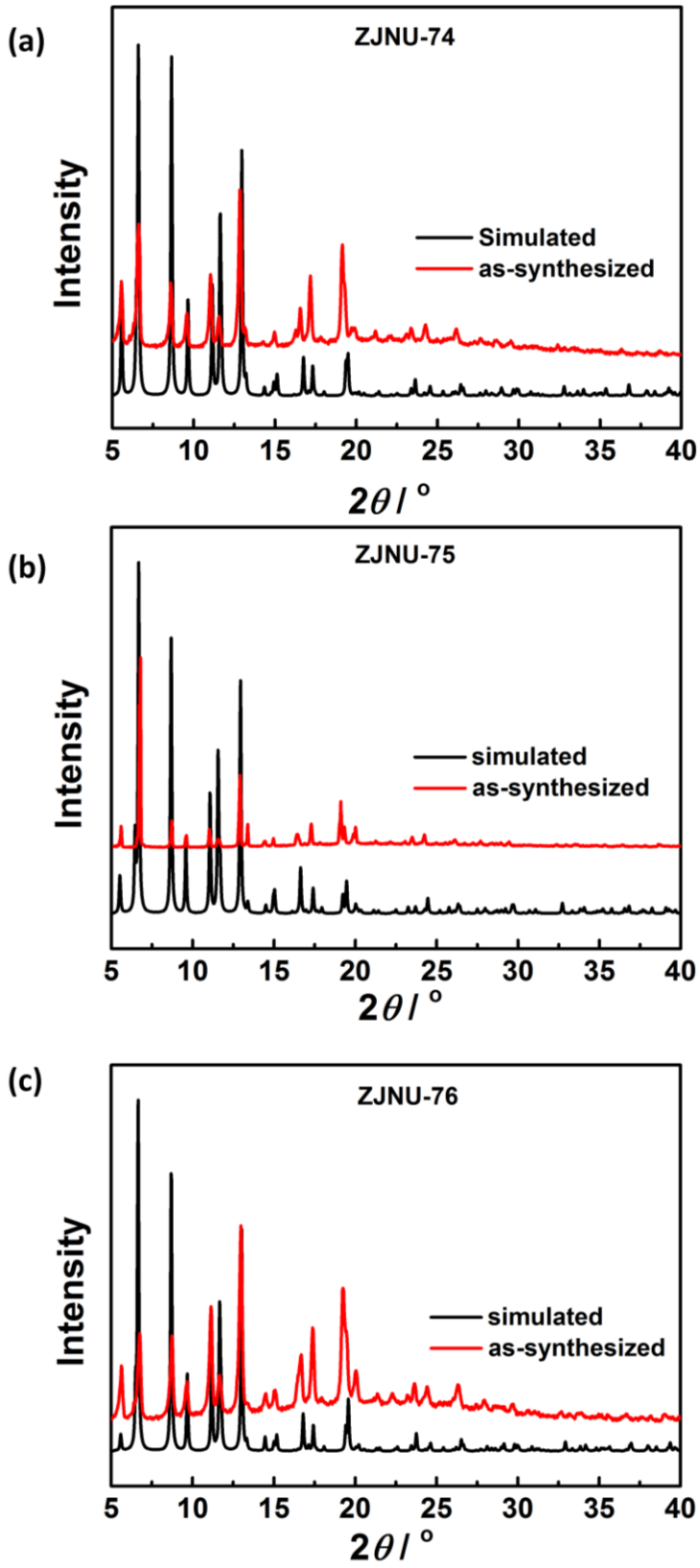

Fig. S1 Comparison of the experimental (red) and simulated (black) PXRD patterns for (a) **ZJNU-74**, (b) **ZJNU-75** and (c) **ZJNU-76**.

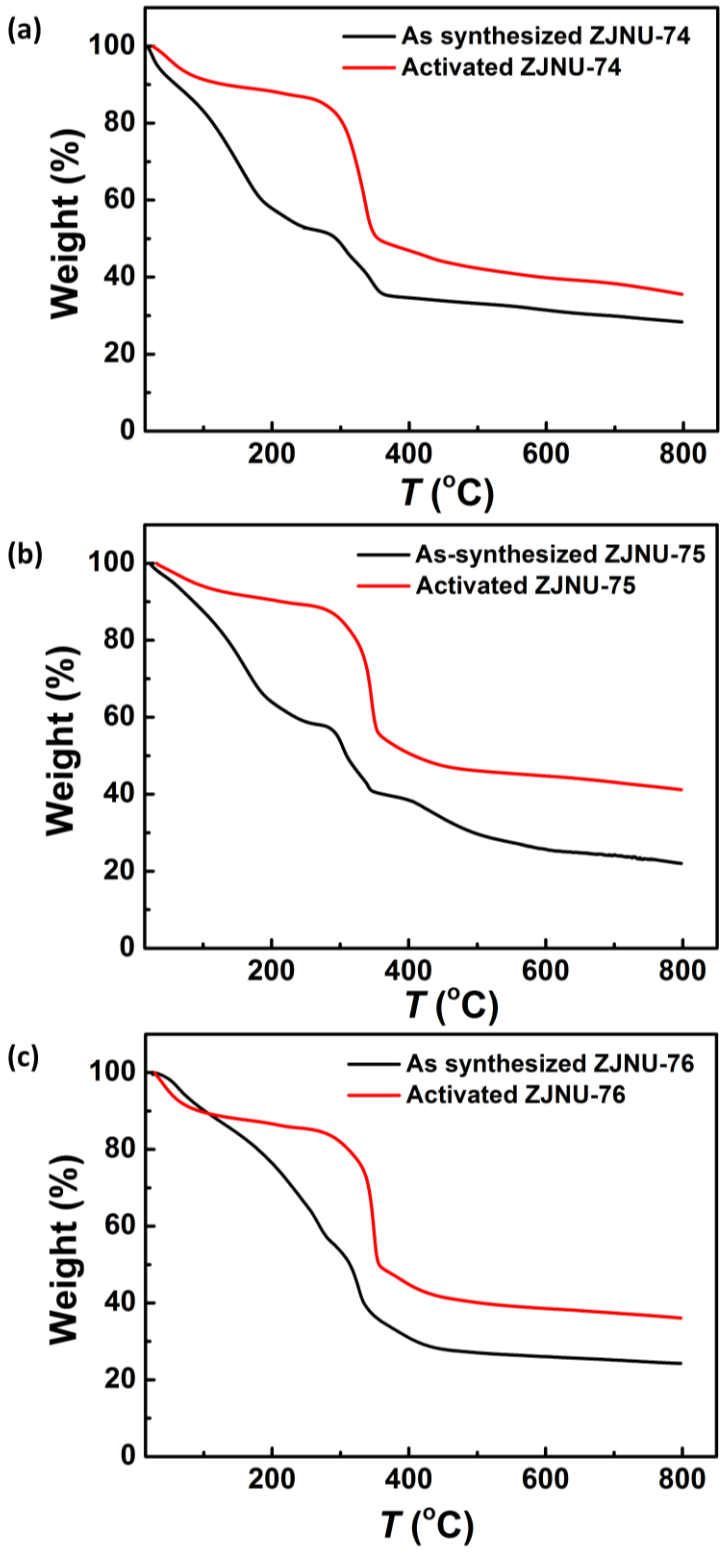

Fig. S2 TGA curves of the as-synthesized and activated (a) **ZJNU-74**, (b) **ZJNU-75** and (c) **ZJNU-76** under nitrogen atmosphere.

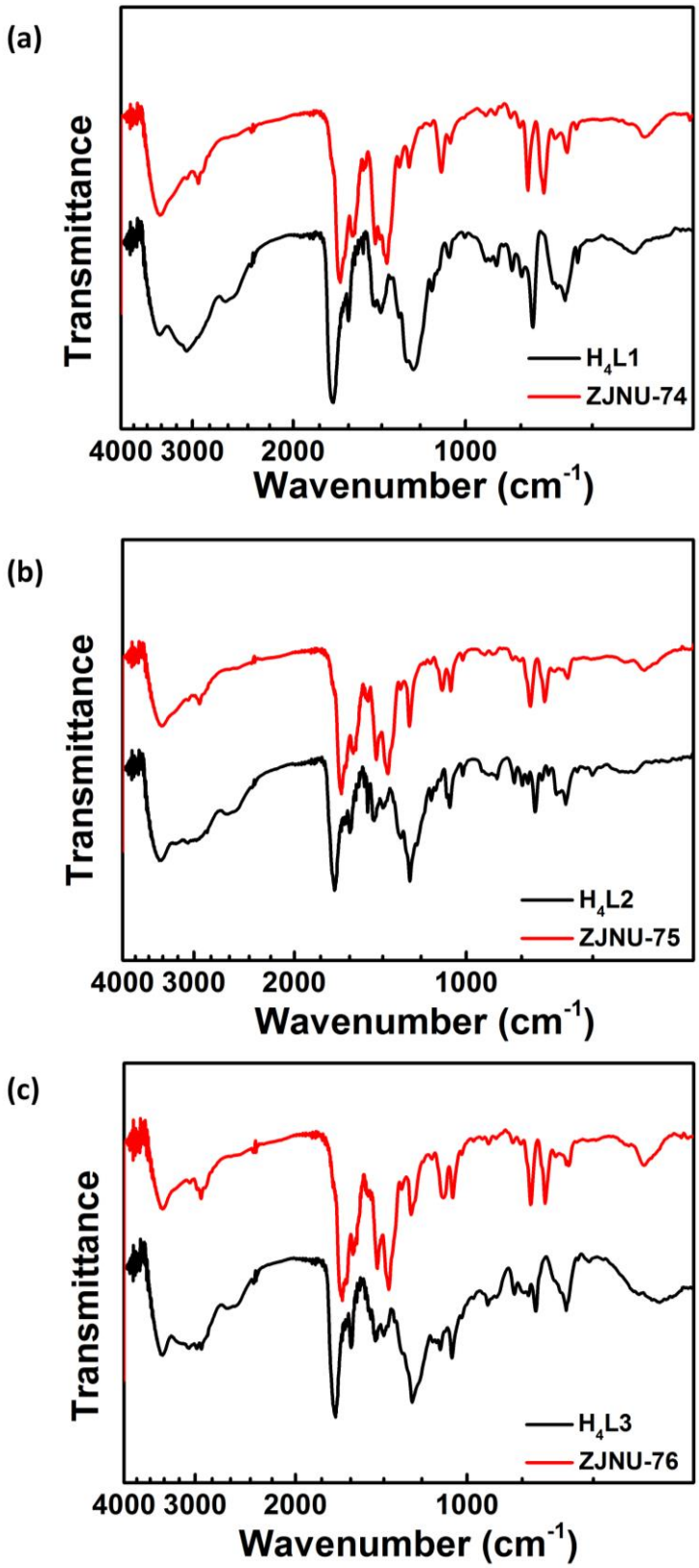

Fig. S3 Comparison of the FTIR spectra of the as-synthesized MOFs of (a) **ZJNU-74**, (b) **ZJNU-75** and (c) **ZJNU-76** and their corresponding organic ligands.

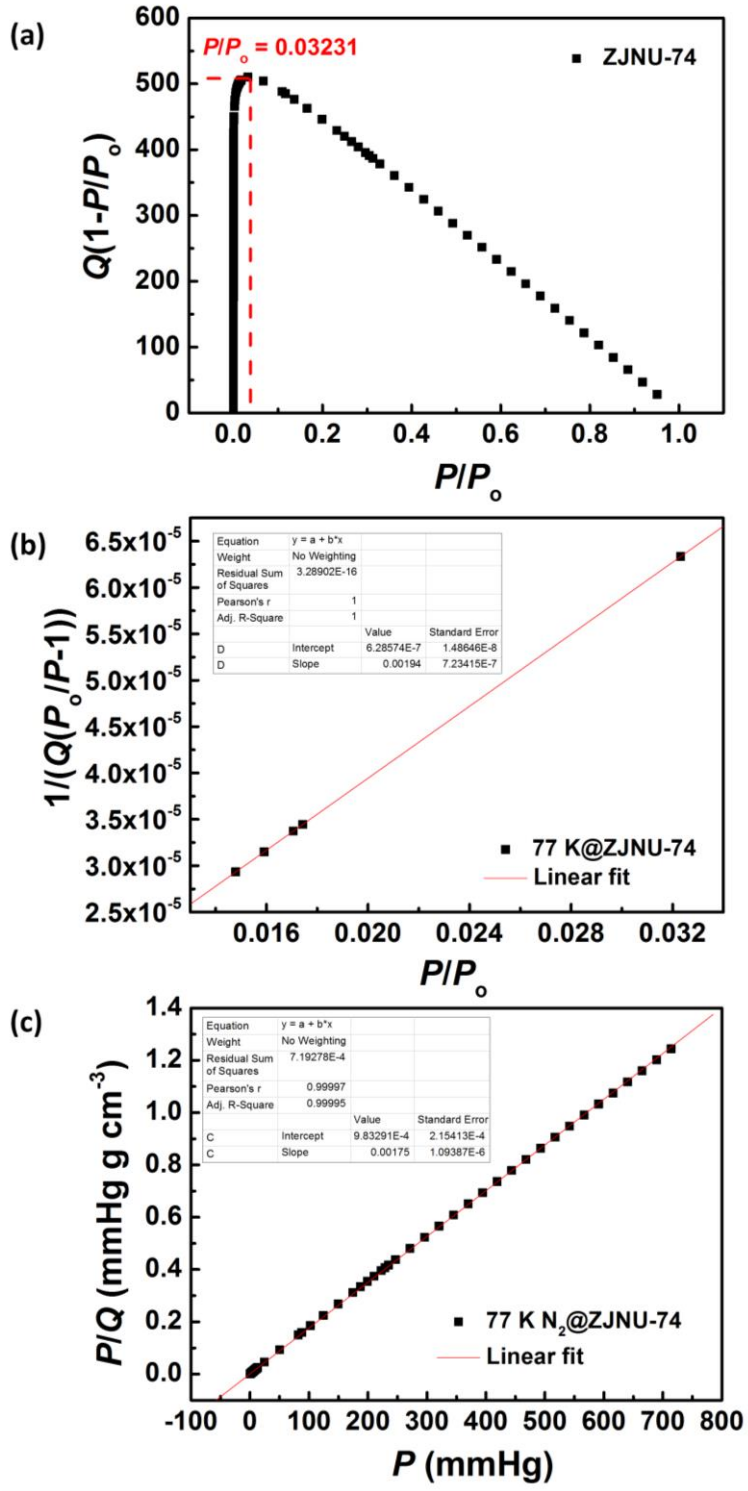

S_{BET} = 1/(6.28574 ×10^{-7} + 0.00194)/22414 × 6.023 × 10^{23} × 0.162 × 10^{-18} = 2243 m^2 g^{-1}

$S_{Langmuir}$ = (1/0.00175)/22414 × 6.023 × 10^{23} × 0.162 × 10^{-18} = 2488 m^2 g^{-1}

BET constant = 1 + 0.00194/6.28574 ×10^{-7} = 3087

Fig. S4 The consistency plot (a), BET plot (b) and Langmuir plot (c) for **ZJNU-74**.

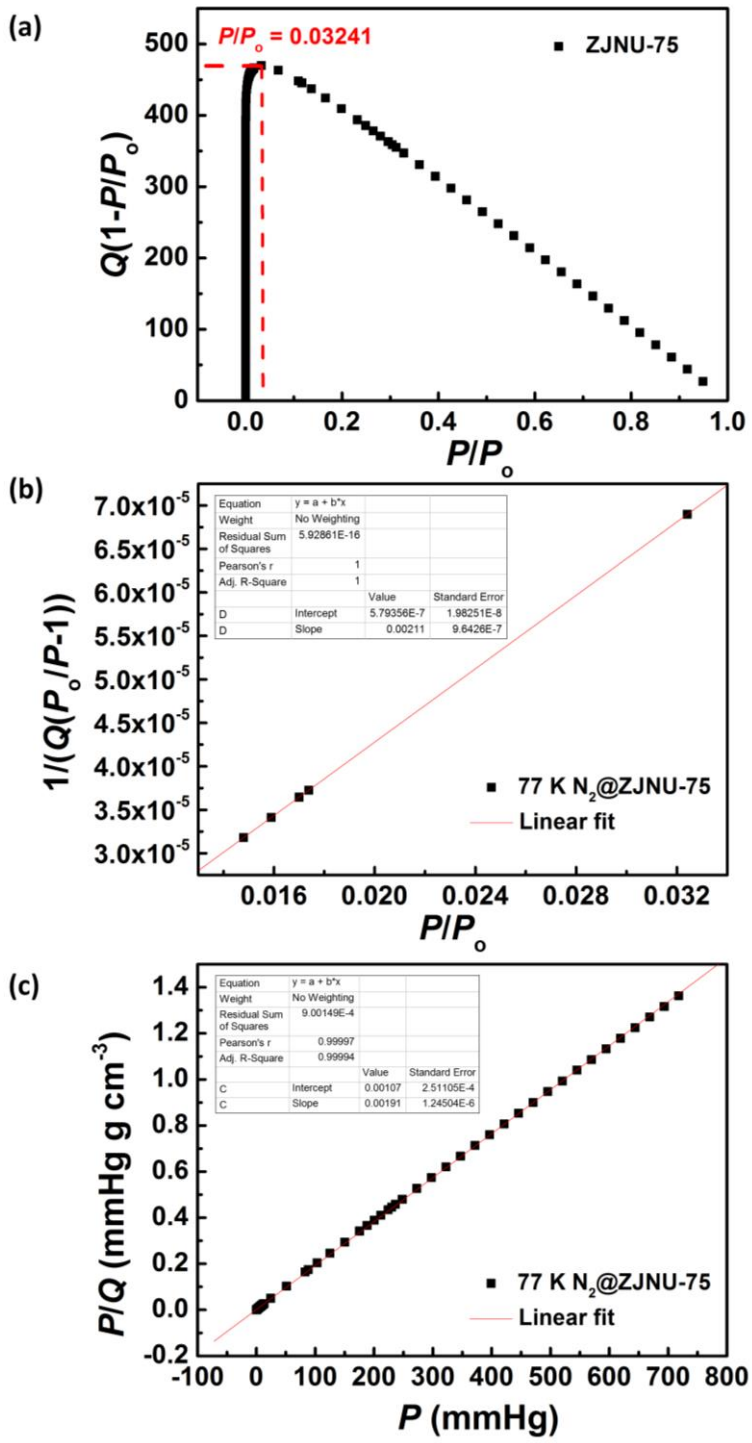

S_{BET} = 1/(5.79356 ×10^{-7}+ 0.00211)/22414 × 6.023 × 10^{23} × 0.162 × 10^{-18} = 2063 m^2 g^{-1}

$S_{Langmuir}$ = (1/0.00191)/22414 × 6.023 × 10^{23} × 0.162 × 10^{-18} = 2279 m^2 g^{-1}

BET constant C = 1 + 0.00211/5.79356 ×10^{-7} = 3643

Fig. S5 The consistency plot (a), BET plot (b) and Langmuir plot (c) for **ZJNU-75**.

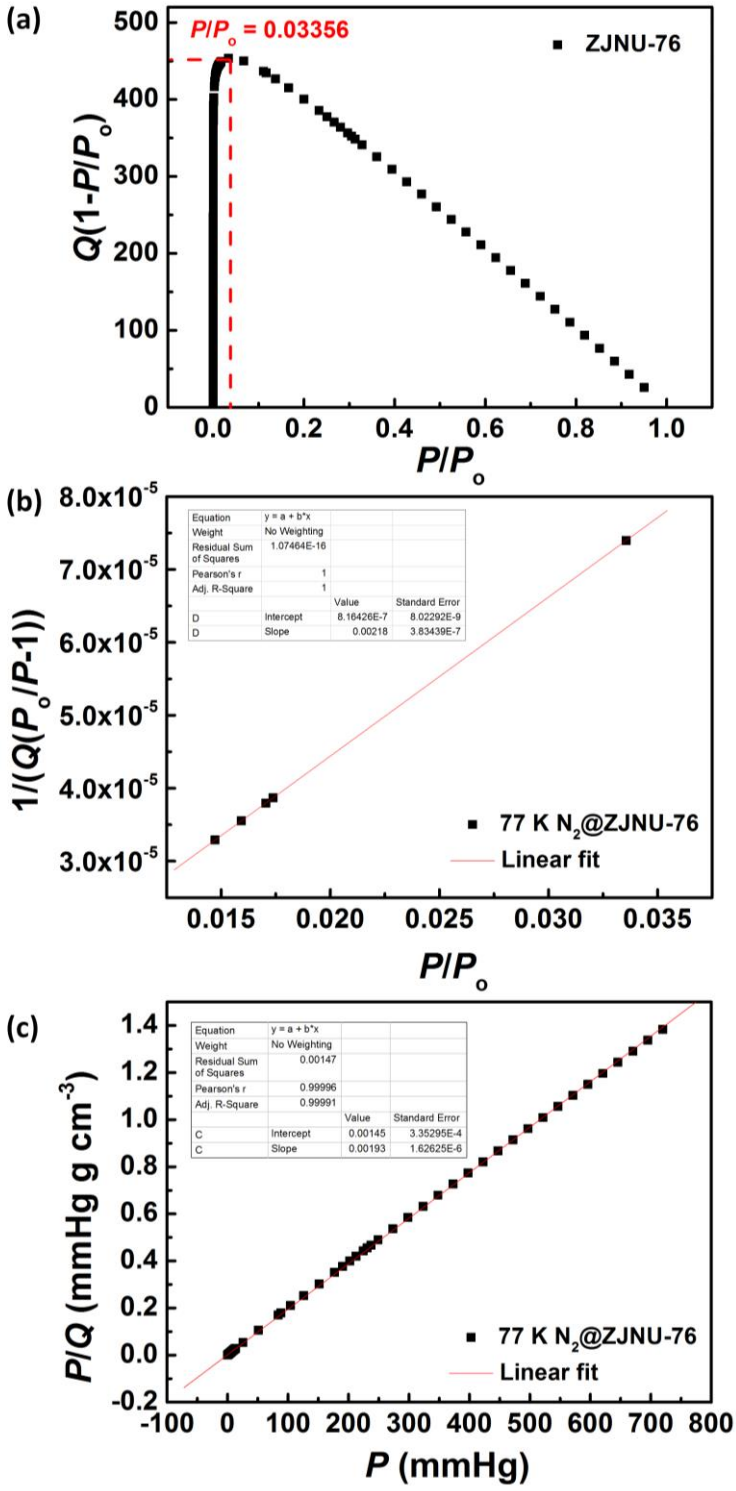

S_{BET} = 1/(8.16426 ×10^{-7}+ 0.00218)/22414 × 6.023 × 10^{23} × 0.162 × 10^{-18} = 1996 m^2 g^{-1}

$S_{Langmuir}$ = (1/0.00193)/22414 × 6.023 × 10^{23} × 0.162 × 10^{-18} = 2256 m^2 g^{-1}

BET constant C = 1 + 0.00218/8.16426 ×10^{-7} = 2671

Fig. S6 The consistency plot (a), BET plot (b) and Langmuir plot (c) for **ZJNU-76**.

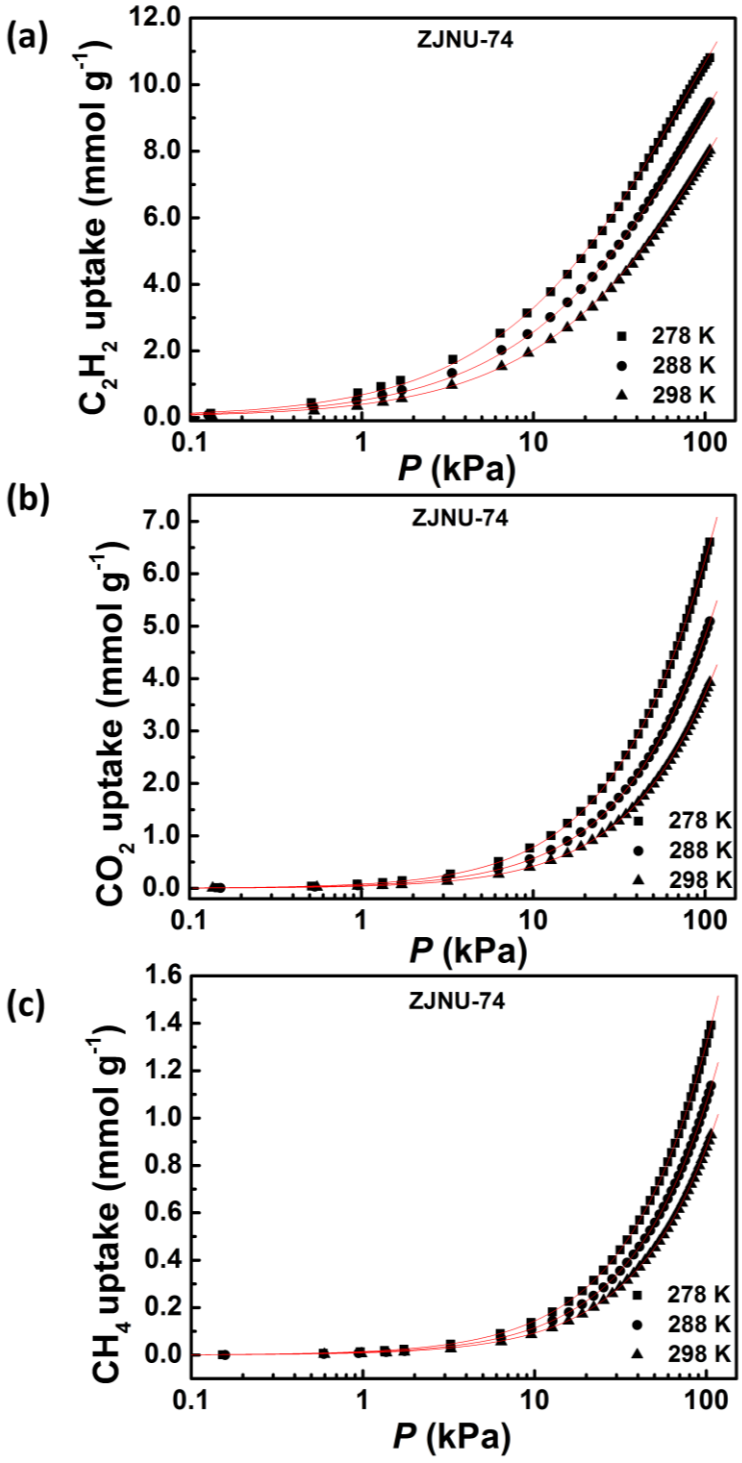

Fig. S7 Comparison of the pure-component isotherm data for (a) C_2H_2, (b) CO_2, and (c) CH_4 in **ZJNU-74** with the fitted isotherms (shown by continuous solid lines) at 278 K, 288 K and 298 K.

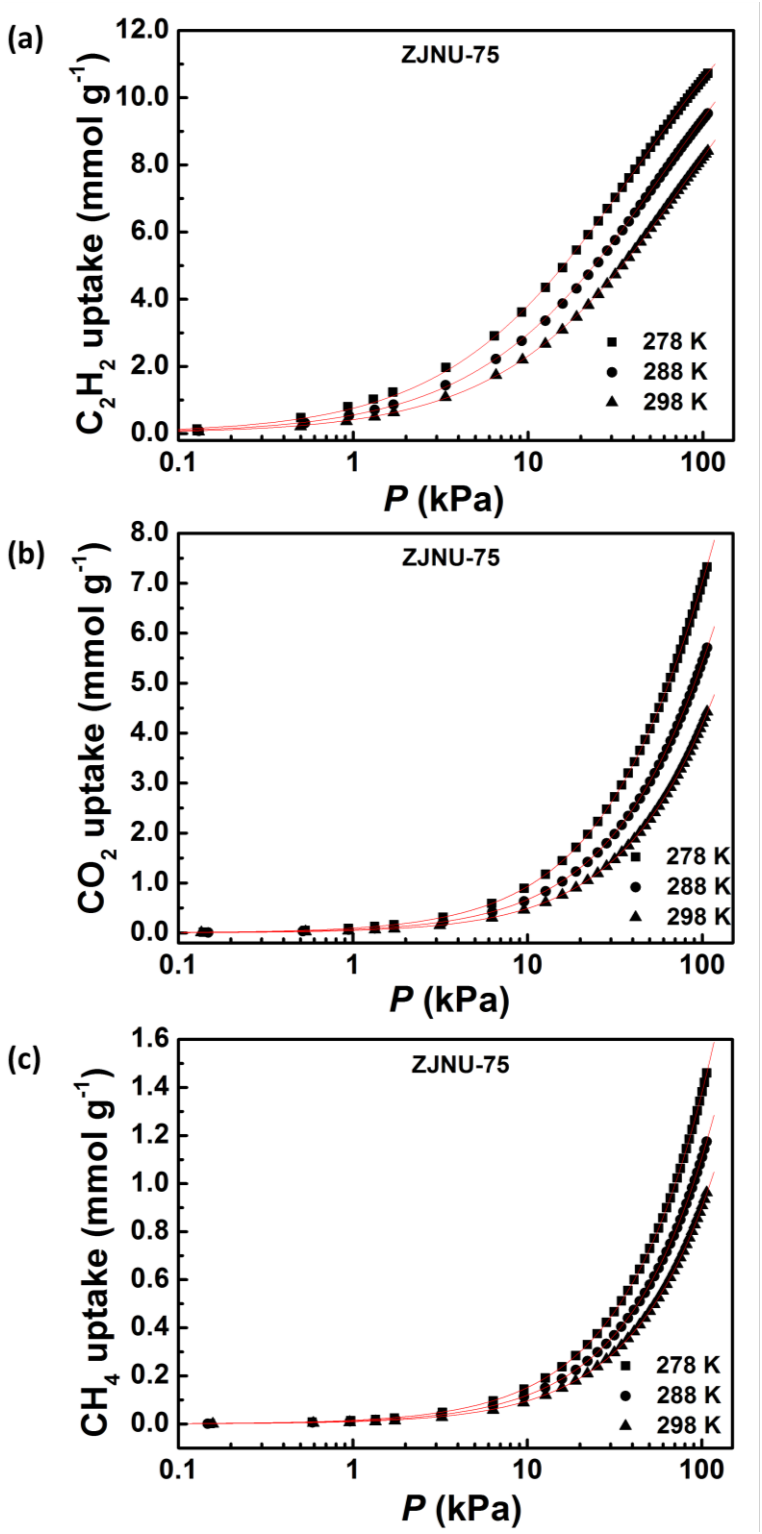

Fig. S8 Comparison of the pure-component isotherm data for (a) C_2H_2, (b) CO_2, and (c) CH_4 in **ZJNU-75** with the fitted isotherms (shown by continuous solid lines) at 278 K, 288 K and 298 K.

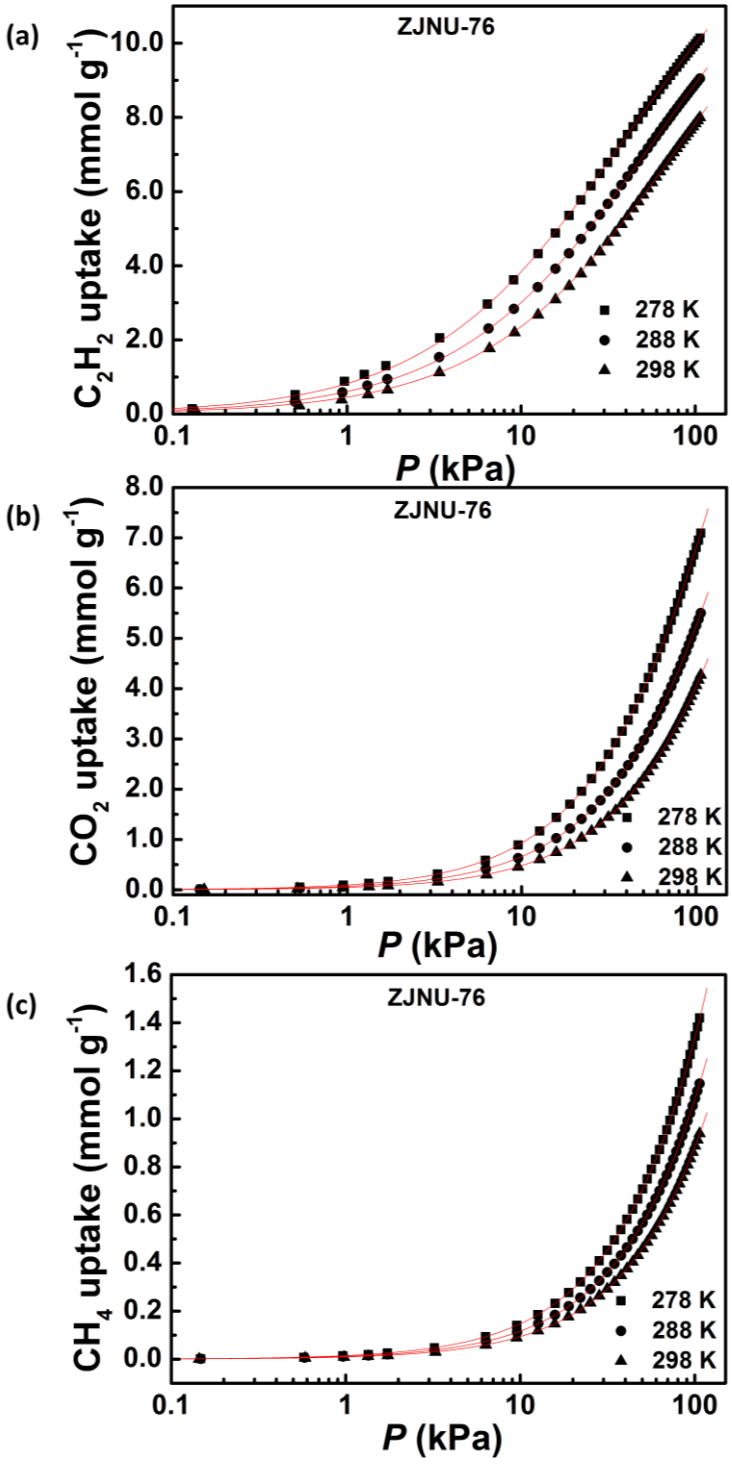

Fig. S9 Comparison of the pure-component isotherm data for (a) C_2H_2, (b) CO_2, and (c) CH_4 in **ZJNU-76** with the fitted isotherms (shown by continuous solid lines) at 278 K, 288 K and 298 K.

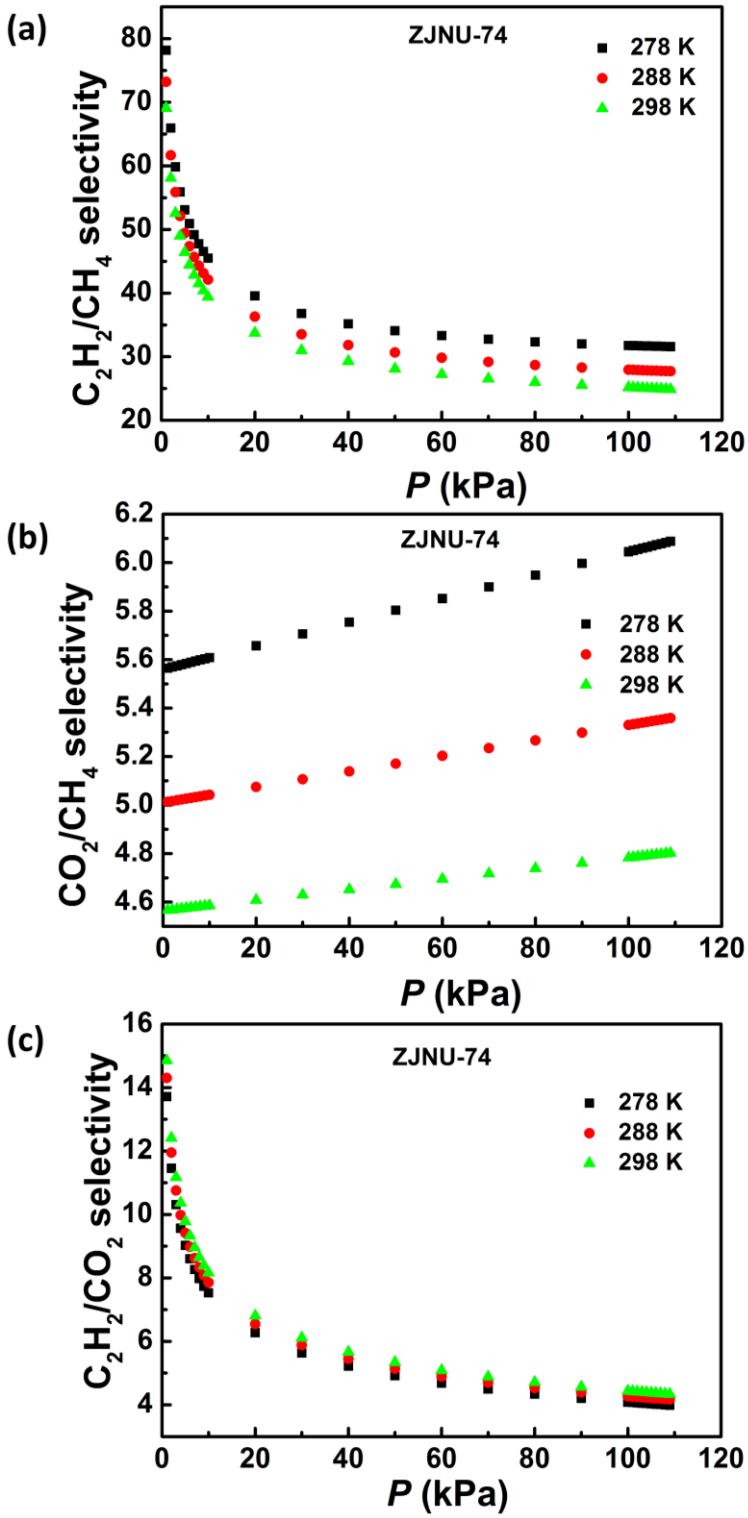

Fig. S10 IAST selectivities for the equimolar (a) C_2H_2/CH_4, (b) CO_2/CH_4 and (c) C_2H_2/CO_2 gas mixtures in **ZJNU-74** at three different temperatures

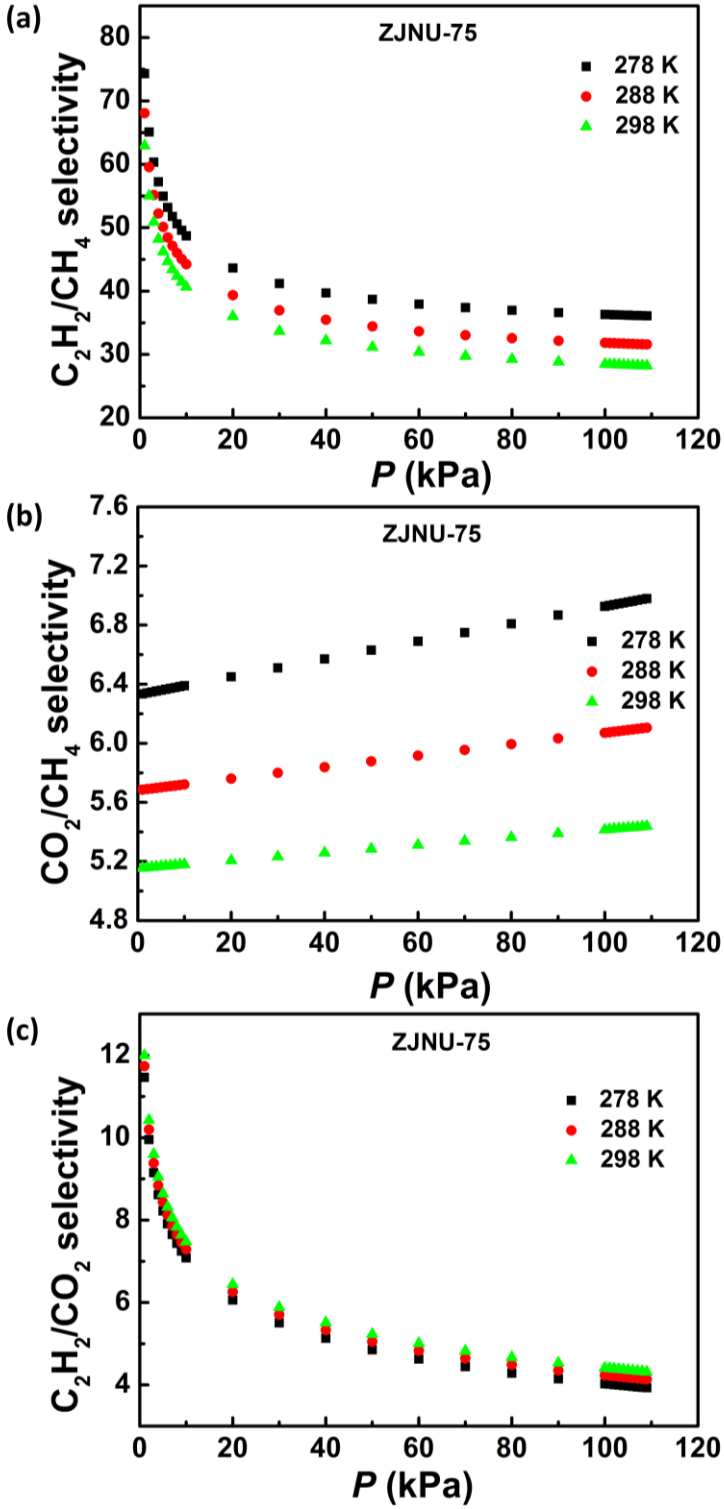

Fig. S11 IAST selectivities for the equimolar (a) C_2H_2/CH_4, (b) CO_2/CH_4 and (c) C_2H_2/CO_2 gas mixtures in **ZJNU-75** at three different temperatures

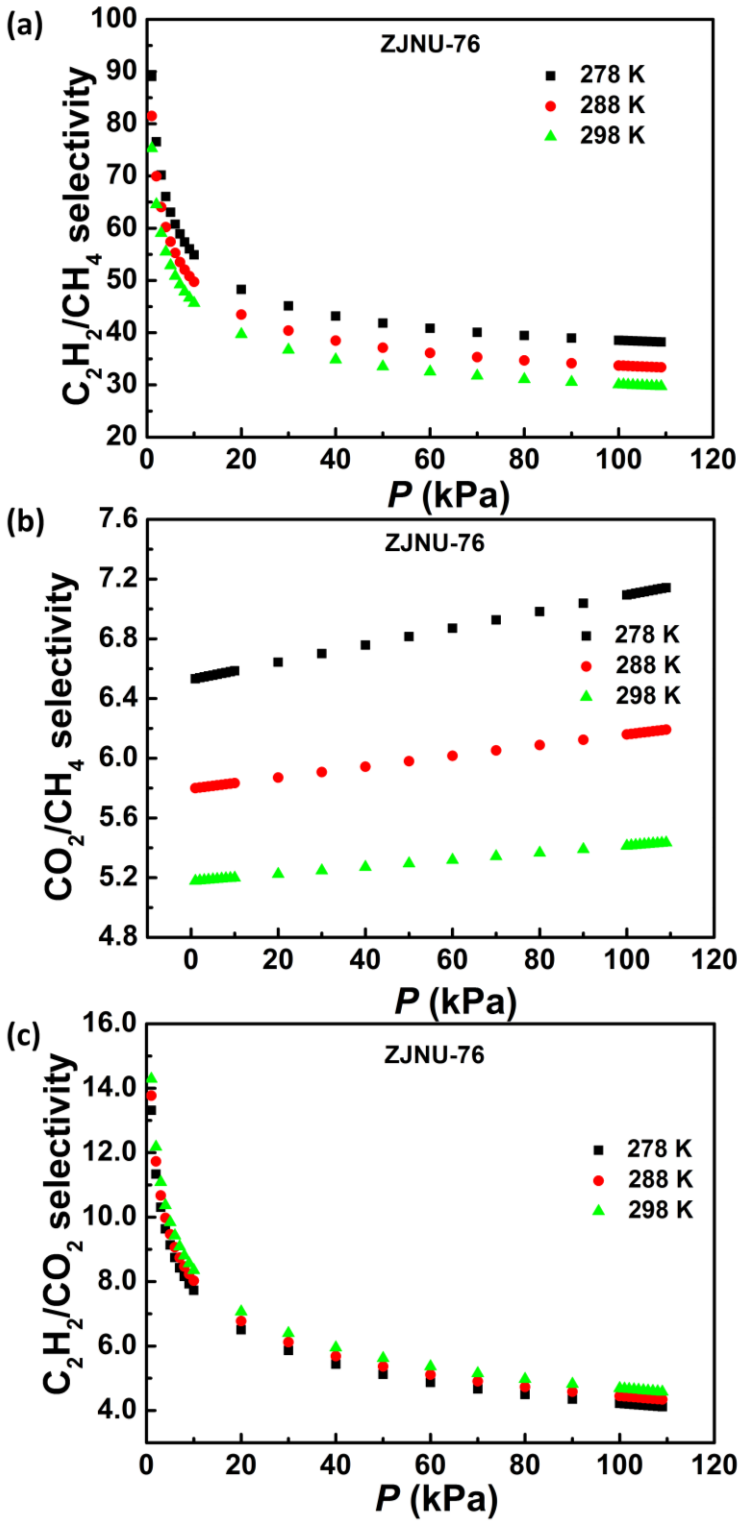

Fig. S12 IAST selectivities for the equimolar (a) C_2H_2/CH_4, (b) CO_2/CH_4 and (c) C_2H_2/CO_2 gas mixtures in **ZJNU-76** at three different temperatures

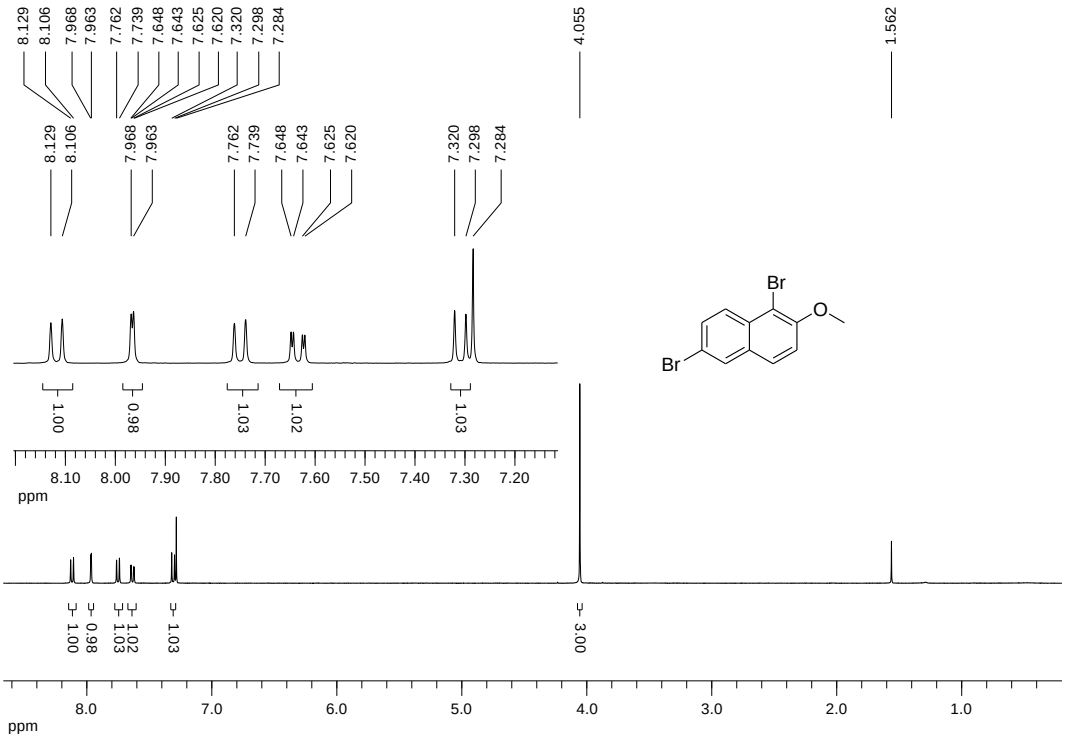
8.129
8.106
7.968
7.963
7.762
7.739
7.648
7.643
7.625
7.620
7.320
7.298
7.284
4.055
1.562
Br
O
Br
1.00
0.98
1.03
1.02
1.03
3.00
ppm

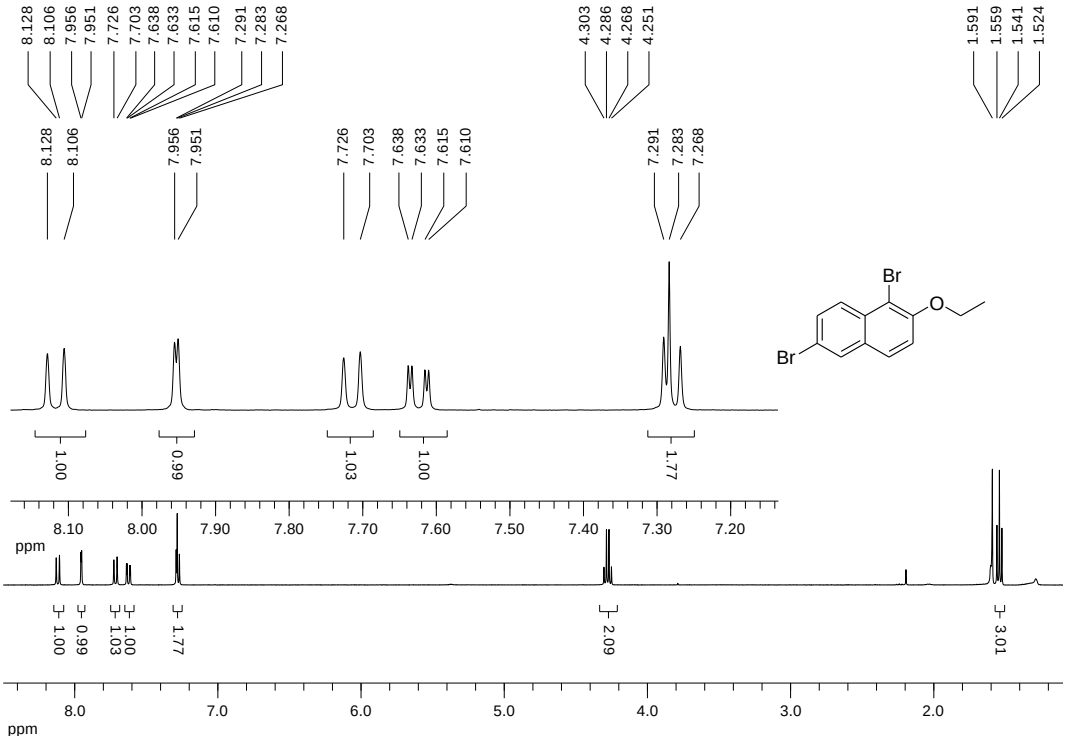
8.128
8.106
7.956
7.951
7.726
7.703
7.638
7.633
7.615
7.610
7.291
7.283
7.268
4.303
4.286
4.268
4.251
1.591
1.559
1.541
1.524
Br
O
Br
1.00
0.99
1.03
1.00
1.77
2.09
3.01
ppm

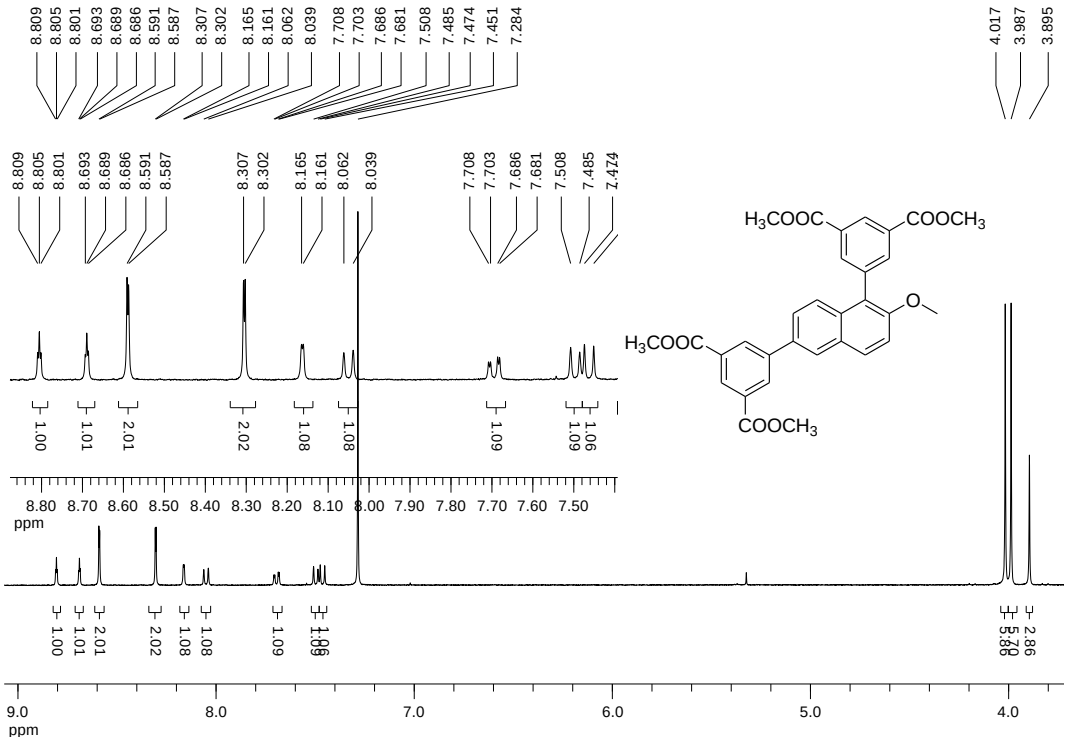
8.809
8.805
8.801
8.693
8.689
8.686
8.591
8.587
8.307
8.302
8.165
8.161
8.062
8.039
7.708
7.703
7.686
7.681
7.508
7.485
7.474
7.451
7.284
4.017
3.987
3.895
1.00
1.01
2.01
2.02
1.08
1.08
1.09
1.09
1.06
2.86
H3COOC
COOCH3
O
H3COOC
COOCH3
8.80 8.70 8.60 8.50 8.40 8.30 8.20 8.10 8.00 7.90 7.80 7.70 7.60 7.50
ppm
9.0
8.0
7.0
6.0
5.0
4.0
ppm

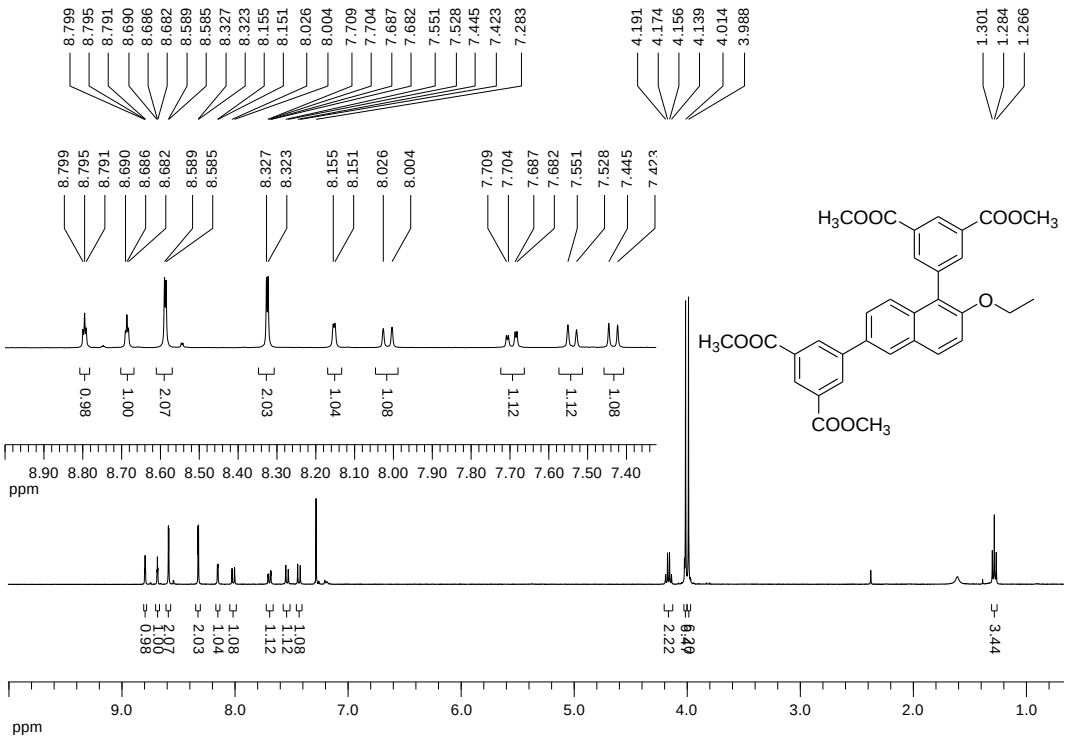
8.799
8.795
8.791
8.690
8.686
8.682
8.589
8.585
8.327
8.323
8.155
8.151
8.026
8.004
7.709
7.704
7.687
7.682
7.551
7.528
7.445
7.423
7.283
4.191
4.174
4.156
4.139
4.014
3.988
1.301
1.284
1.266
0.98
1.00
2.07
2.03
1.04
1.08
1.12
1.12
1.08
2.22
3.44
H3COOC
COOCH3
O
H3COOC
COOCH3
8.90 8.80 8.70 8.60 8.50 8.40 8.30 8.20 8.10 8.00 7.90 7.80 7.70 7.60 7.50 7.40
ppm
9.0
8.0
7.0
6.0
5.0
4.0
3.0
2.0
1.0
ppm

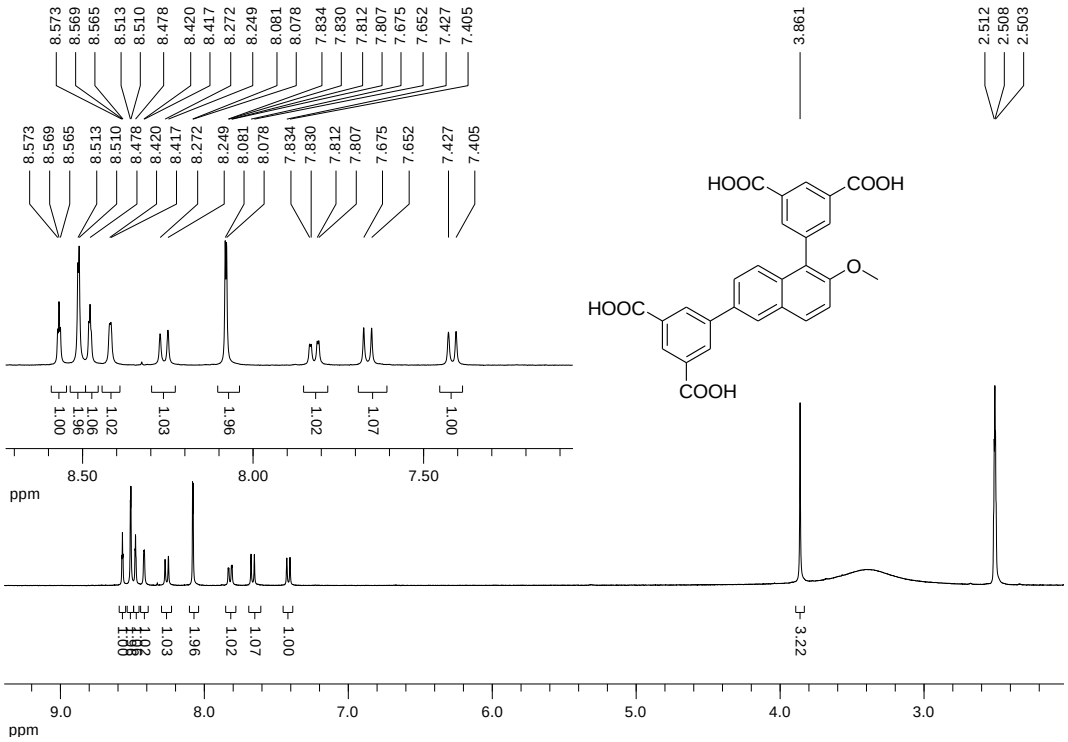
8.573
8.569
8.565
8.513
8.510
8.478
8.420
8.417
8.272
8.249
8.081
8.078
7.834
7.830
7.812
7.807
7.675
7.652
7.427
7.405
3.861
2.512
2.508
2.503
HOOC
COOH
O
HOOC
COOH
1.00
1.96
1.06
1.02
1.03
1.96
1.02
1.07
1.00
3.22
ppm

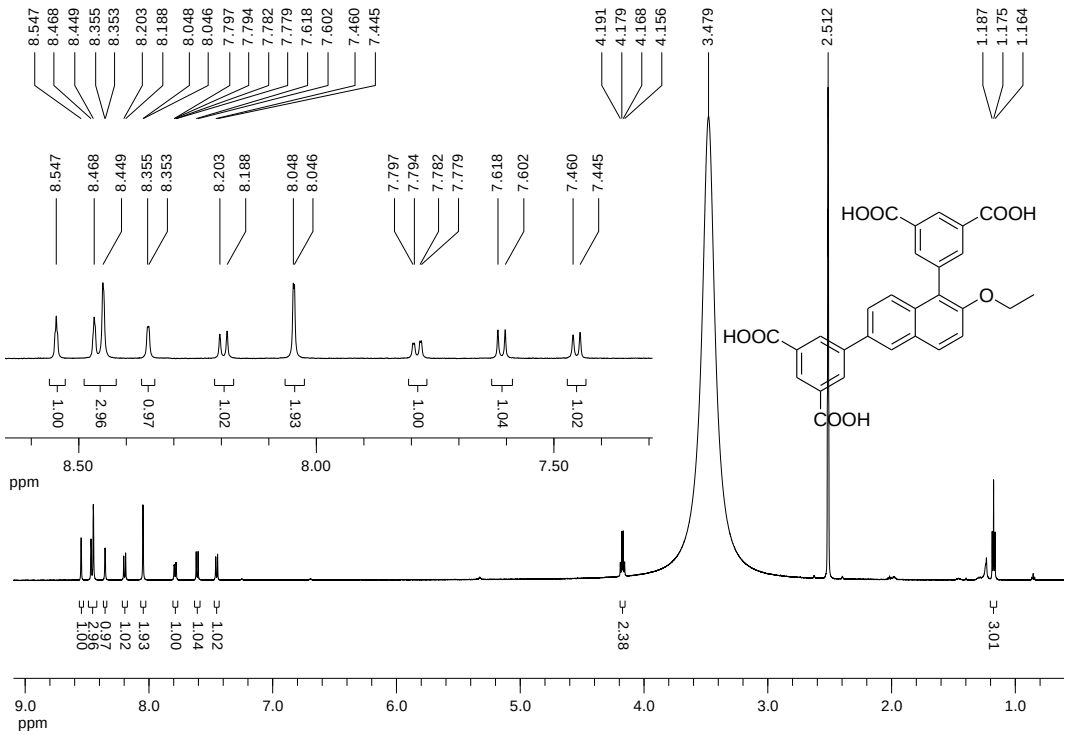
8.547
8.468
8.449
8.355
8.353
8.203
8.188
8.048
8.046
7.797
7.794
7.782
7.779
7.618
7.602
7.460
7.445
4.191
4.179
4.168
4.156
3.479
2.512
1.187
1.175
1.164
HOOC
COOH
O
HOOC
COOH
1.00
2.96
0.97
1.02
1.93
1.00
1.04
1.02
2.38
3.01
ppm

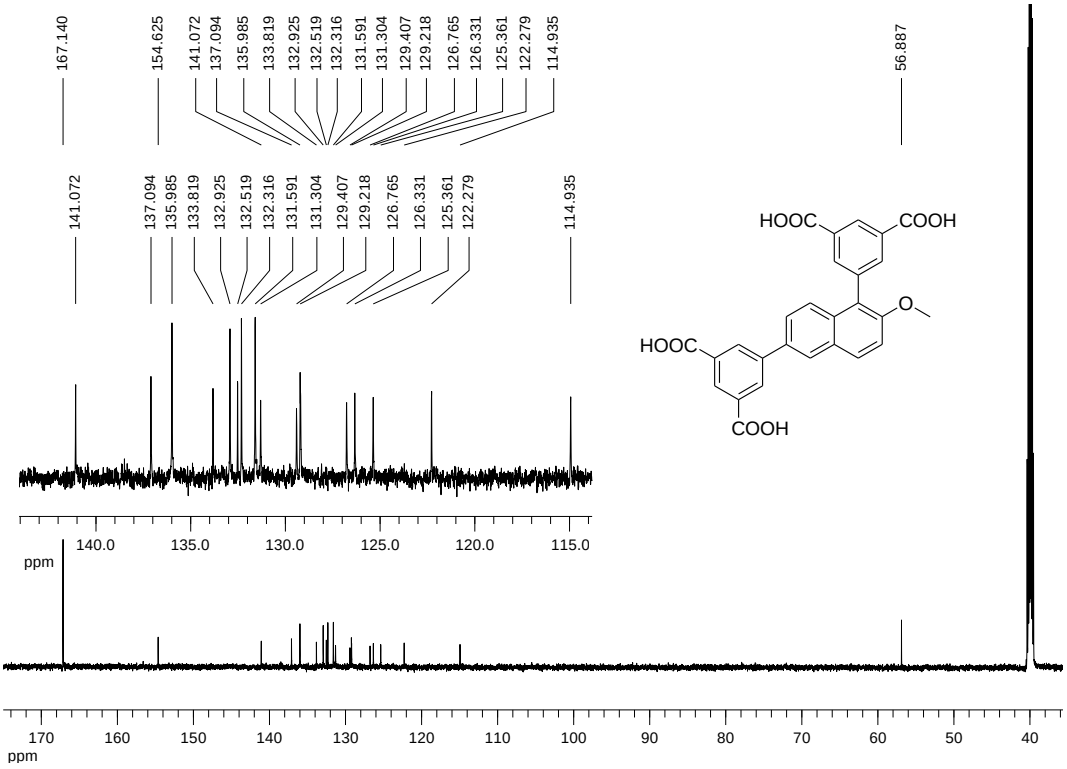

Fig. S13 ^{1}H and ^{13}C NMR spectra

Table S1 Langmuir-Freundich parameters for adsorption of C_2H_2, CO_2, and CH_4 in **ZJNU-74**.

	q_{sat} (mmol g^{-1})	b_0 $(kPa)^{-v}$	E (kJ mol^{-1})	v
C_2H_2	20.91231	8.40333×10^{-6}	19.17	0.74571
CO_2	28.25702	2.3211×10^{-7}	21.76	1
CH_4	13.79579	1.4927×10^{-6}	15.16	1

Table S2 Langmuir-Freundich parameters for adsorption of C_2H_2, CO_2, and CH_4 in **ZJNU-75**.

	q_{sat} (mmol g^{-1})	b_0 $(kPa)^{-v}$	E (kJ mol^{-1})	v
C_2H_2	15.77432	4.93489×10^{-6}	21.33	0.80314
CO_2	25.69717	2.02268×10^{-7}	22.72	1
CH_4	13.63143	1.191×10^{-6}	15.83	1

Table S3 Langmuir-Freundich parameters for adsorption of C_2H_2, CO_2, and CH_4 in **ZJNU-76**.

	q_{sat} (mmol g^{-1})	b_0 $(kPa)^{-v}$	E (kJ mol^{-1})	v
C_2H_2	14.73308	6.35303×10^{-6}	21.12	0.77478
CO_2	22.70595	1.71438×10^{-7}	23.40	1
CH_4	13.14488	1.33364×10^{-6}	15.59	1

Table S4 Crystal data and structure refinement for **ZJNU-74**, **ZJNU-75** and **ZJNU-76**.

MOFs	**ZJNU-74**	**ZJNU-75**	**ZJNU-76**
Empirical formula	$C_{26}H_{16}O_{10}$ Cu_2	$C_{27}H_{18}O_{11}Cu_2$	$C_{28}H_{20}O_{11}Cu_2$
Formula weight	615.47	645.49	659.52
λ (Å)	1.54184	1.54184	1.54178
Crystal system	Hexagonal	Hexagonal	Hexagonal
Space group	$P6_3/mmc$	$P6_3/mmc$	$P6_3/mmc$
Unit cell dimensions	a = 18.3150(7) Å b = 18.3150(7) Å c = 26.7665(14) Å α = 90° β = 90° γ = 120°	a = 18.4455(6) Å b = 18.4455(6) Å c = 26.4268(5) Å α = 90° β = 90° γ = 120°	a = 18.2664(5) Å b = 18.2664(5) Å c = 26.5488(6) Å α = 90° β = 90° γ = 120°
V (Å^3)	7775.6(6)	7786.7(4)	7671.5(3)
Z	6	6	6
D_c (g cm^{-3})	0.789	0.826	0.857
μ (mm^{-1})	1.260	1.289	1.315
F(000)	1860	1956	2004
Crystal size (mm)	0.23 × 0.15 × 0.10	0.23 × 0.18 × 0.17	0.23 × 0.12 × 0.10
θ range for data collection (°)	4.32 to 74.00	3.34 to 73.91	4.35 to 73.86
Limiting indices	$-20 \le h \le 13$ $-15 \le k \le 22$ $-32 \le l \le 27$	$-22 \le h \le 16$ $-16 \le k \le 22$ $-32 \le l \le 28$	$-8 \le h \le 22$ $-17 \le k \le 15$ $-31 \le l \le 32$
Reflections collected / unique	23259 / 2907	28201 / 2942	17309 / 2848
R_{int}	0.0574	0.0382	0.0459
Max. and min. transmission	0.8844 and 0.7604	0.8107 and 0.7559	0.8797 and 0.7519
Refinement method	Full-matrix least-squares on F^2	Full-matrix least-squares on F^2	Full-matrix least-squares on F^2
Data/restraints/parameters	2907 / 103 / 119	2942 / 145 / 143	2848 / 265 / 161
Goodness-of-fit on F^2	1.044	1.030	1.643
Final R indices [$I > 2\sigma(I)$]	R_1 = 0.1425 wR_2 = 0.4061	R_1 = 0.1593 wR_2 = 0.5094	R_1 = 0.1510 wR_2 = 0.4674
R indices (all data)	R_1 = 0.2137 wR_2 = 0.4543	R_1 = 0.1875 wR_2 = 0.5563	R_1 = 0.1928 wR_2 = 0.4955
Largest diff. peak and hole (e.Å^{-3})	0.545 and -0.604	0.859 and -0.670	0.581 and -0.487
CCDC	1558048	1558537	1543094

(1) **Fitting of Pure-Component Isotherms**

The pure-component C_2H_2, CO_2 and CH_4 adsorption isotherms measured at 278 K, 288 K and 298 K were fitted with the single-site Langmuir-Freundlich model

$$q = \frac{q_{sat} b p^{v}}{1 + b p^{v}}$$, with *T*-dependent parameter $$b = b_o \exp(\frac{E_a}{RT})$$

where q is the adsorbed amount (mmol g^{-1}), q_{sat} is the monolayer adsorption capacity (mmol g^{-1}), p is the equilibrium pressure (kPa), and b and v is the Langmuir and Freundlich constants. The corresponding fitting parameters are provided in Table S1-3. Fig. S7 provides a comparison of the experimental isotherm data for C_2H_2, CO_2 and CH_4 in **ZJNU-74** with the isotherm fits. Fig. S8 provides a comparison of the experimental isotherm data for C_2H_2, CO_2 and CH_4 in **ZJNU-75** with the isotherm fits. Fig. S9 provides a comparison of the experimental isotherm data for C_2H_2, CO_2 and CH_4 in **ZJNU-76** with the isotherm fits.

(2) **IAST calculations of adsorption selectivities**

The selectivity of preferential adsorption of component 1 over component 2 in a mixture containing 1 and 2 can be formally defined as

$$S_{\text{ads}} = \frac{q_1 / q_2}{p_1 / p_2}$$

q_1 and q_2 are the absolute component loadings of the adsorbed phase in the mixture. These component loadings are also termed the uptake capacities. We calculated the values of q_1 and q_2 using the IAST of Myers and Prausnitz (Ref. A. L. Myers and J. M. Prausnitz, *A.I.Ch.E.J.*, **1965**, *11*, 121-127).

(3) **Calculation of Isosteric Heats of Adsorption**

The isosteric heats of adsorption (Q_{st}) were calculated using the Clausius-Clapeyron equation based on pure-component isotherms collected at three different temperatures of 278 K, 288 K and 298 K. The Q_{st} was defined as

$$Q_{st} = -R \left(\frac{\partial Inp}{\partial (1/T)} \right)_q$$

where p is the pressure, T is the temperature, R is the gas constant, and q is the adsorption amount. These calculations were done through the "Heat of Adsorption" function embedded in the software supplied by Micromeritics ASAP 2020 HD88 surface-area and pore-size analyzer machine.